Thermal management of standby battery for outdoor base station based on the semiconductor thermoelectric device and phase change materials

Song, Wenji; Bai, Fanfei; Chen, Mingbiao; Lin, Shili; Feng, Ziping; Li, Yongliang

DOI:
10.1016/j.applthermaleng.2018.03.072

Document Version
Peer reviewed version

Citation for published version (Harvard):
Song, W, Bai, F, Chen, M, Lin, S, Feng, Z & Li, Y 2018, 'Thermal management of standby battery for outdoor base station based on the semiconductor thermoelectric device and phase change materials', *Applied Thermal Engineering*, vol. 137, pp. 203-217. https://doi.org/10.1016/j.applthermaleng.2018.03.072

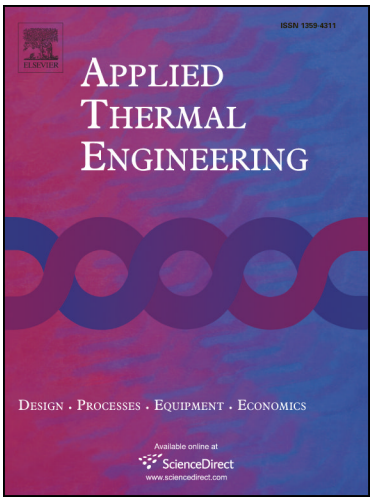

Thermal management of standby battery for outdoor base station based on the semiconductor thermoelectric device and phase change materials

Wenji Song, Fanfei Bai, Mingbiao Chen, Shili Lin, Ziping Feng, Yongliang Li

PII: S1359-4311(18)30951-7
DOI: https://doi.org/10.1016/j.applthermaleng.2018.03.072
Reference: ATE 11960

To appear in: *Applied Thermal Engineering*

Received Date: 10 February 2018
Revised Date: 14 March 2018
Accepted Date: 20 March 2018

Please cite this article as: W. Song, F. Bai, M. Chen, S. Lin, Z. Feng, Y. Li, Thermal management of standby battery for outdoor base station based on the semiconductor thermoelectric device and phase change materials, *Applied Thermal Engineering* (2018), doi: https://doi.org/10.1016/j.applthermaleng.2018.03.072

Thermal management of standby battery for outdoor base station based on the semiconductor thermoelectric device and phase change materials

Wenji Song,[a,b,c] Fanfei Bai,[a,b,c,d]* Mingbiao Chen,[a,b,c] Shili Lin,[a,b,c,d] Ziping Feng,[a,b,c] Yongliang Li,[e]

[a]Guangzhou Institute of Energy Conversion, Chinese Academy of Sciences, Guangzhou 510640, China

[b]CAS Key Laboratory of Renewable Energy, Chinese Academy of Sciences, Guangzhou 510640, China

[c]Guangdong Provincial Key Laboratory of New and Renewable Energy Research and Development, Guangzhou 510640, China

[d]University of Chinese Academy of Sciences, Beijing 10049, China

[e]School of Chemical Engineering, University of Birmingham, Birmingham B15 2TT, United Kingdom

The following is the e-mail of authors:

1) Name: Wenji Song E-mail: songwj@ms.giec.ac.cn

2) Name: Fanfei Bai* E-mail: baiff@ms.giec.ac.cn

3) Name: Mingbiao Chen E-mail: chenmb@ms.giec.ac.cn

4) Name: Shili Lin E-mail: linsl@ms.giec.ac.cn

5) Name: Ziping Feng E-mail: fengzp@ms.giec.ac.cn

6) Name: Yongliang Li E-mail: y.li.1@bham.ac.uk

Highlights：

Thermal management based on the semiconductor thermoelectric device and PCMs was proposed.

The management can cool/heat the battery module and keep its temperature in optimal range.

The management was effective in different ambient temperature and discharge-charge process.

The performance was stable in continuous cooling / heating –heat preservation cycle.

Abstract： In order to extend the life span of standby battery for outdoor base station, a semiconductor thermoelectric device / phase change materials (PCMs) coupled battery thermal management system (BTMS), as well as the three-dimensional model of 48V 80Ah battery pack, was designed in this paper. The effect of various influencing factors, especially semiconductor thermoelectric device arrangement, temperature range of thermal management, cooling and heating power was investigated numerically. The results showed that the semiconductor thermoelectric devices were arranged at two flanks of minimum size direction could effectively improve the uniformity of battery module temperature field and prolong the heat preservation process. When the temperature difference between upper or lower limit of thermal management temperature range and the phase change temperature of PCMs (T_{PCM}) was no more than 5K, the maximum temperature difference (ΔT_{max}) of battery module during the cooling or heating process was lower than 5K. Both the best choice of cooling and heating power was 200 W. What's more, after 1C discharging and 0.5C charging process, the maximum temperature ($T_{\max}$) of battery module was restrained under the 312K. During continuous cooling and heat preservation cycle, the cooling time and heat preservation time was about 14 hours and 4.15 days, respectively, when the average ambient temperature was 323K. The simulation results will be useful for the design of PCMs based battery thermal management system for outdoor base station battery.

Keywords： Semiconductor thermoelectric device; Phase change materials; Battery thermal management

Nomenclature

t	time (s)	Gr	Grashof number
T_{max}	maximum temperature (K)	Nu	Nusselt number
T_{min}	minimum temperature (K)	Pr	Prandtl Number
ΔT_{max}	maximum temperature difference (K)	**Greek symbols**	
T_{PCM}	phase change temperature of PCMs	a	Seebeck coefficients (V / K)
T	temperature (K)	β	cubical expansion coefficient
c_p	specific heat (J/(kg K))	γ	volume fraction
q	heat (J)	υ	viscosity (kg/(m s))
C	constant	ρ	density (kg/m)
l	characteristic length (m)	λ	thermal conductivity (W/(m K))
L	latent heat (J/(kg K))	δ	thickness (mm)
R	resistances (Ω)	ε	surface emissivity
H	enthalpy (J/k)	σ	Stefan-Boltzmann constant (J/ K)
ΔG	gibbs free energy change (J/mol)	**Subscripts**	
ΔS	entropy change (J/(mol K))	b	battery
h	heat transfer coefficient (W/(m^2 K))	o	ohm
I	current (A)	p	polarization
E	potential (V)	oc	open circuit
V	volume (m^3)	f	floating charge
u	velocity (m/s)	∞	ambient
g	gravitational acceleration (m/s^2)	in	thermal insulation material

cold	cold end	X	X direction
hot	hot end	Y	Y direction
m	mean	Z	Z direction
PN	PN bulk	**Acronyms**	
N	N-type elements	PCMs	phase change materials
P	P-type elements	BTMS	battery thermal management system
dis	dissipation	SOC	state of charge
out	out surface of battery pack	HEV	hybrid electric vehicle
Al	aluminum	EV	electric vehicle

1. Introduction

With the development of information and communication technology, the number of outdoor base stations gradually increased. Under normal circumstances, the base station is powered by the rectified municipal AC electric network, which is used for floating charging the standby battery pack at the same time. When the base stations lose the off-site power, the standby battery pack provides the power to ensure the regular and continuous duty of communication equipment. Sometimes the DC power equipment is placed in outdoor enclosures as ambient temperature varies from 253K to 333K.

Because of its low price, high safety, life span, and energy density, the lithium iron phosphate battery is widely used in modern battery storage. In the outdoor stationary base stations [1], lithium-ion iron phosphate solutions are chiefly limited to indoor applications because of the rapid

life reduction when placed outside. Typical operational temperature for lithium-ion battery ranges from 293K to 313K. Heat generation during charging or discharging cycles leads to the temperature rising. The heat accumulation may cause the battery overheat or even thermal runaway. And the performances, safety and service life will all be greatly affected [2]. When battery works in subzero temperatures, the kinetics of charge transfer get sluggish. Electrolyte conductivity becomes low and the solid-state Li diffusivity is reduced [3]. All these result in poor performance of li-ion battery module. As the kinetic and transport processes are highly temperature dependent, battery performs better when it is kept warm. Consequently, there is a need for a low-cost, efficient thermal management package that provides an adequate operational temperature range to enable outdoor applications of lithium-ion iron phosphate battery module [4].

At present, the battery thermal management system has been widely used to protect the power battery installed on the hybrid electric vehicle (HEV) and electric vehicle (EV) [5-7]. The frequent charging and discharging with high rate makes the power battery generate large numbers of heat [8-9]. The battery thermal management prevents the temperature rising at hot environment or preheats the battery pack at the cold environment [10]. But the thermal management of outdoor standby battery pack was rarely noticed. In some remote region, the standby battery pack of outdoor base stations operates at low temperature in winter or at high temperature in summer for a long time. It raises the demand of cooling / heating and it keeps heat preservation for a long time. Problem can be solved by burying the battery pack in the earth. But it is complex and unpractical to restructure the station on the existing basis. So the best solution is increasing corresponding auxiliary equipment to keep the battery at proper temperature.

Meng [11] used the refrigeration system to cool the lead-acid based battery used in outdoor

stationary base stations. 24 batteries were arranged as two-layer configuration or six-layer configuration respectively in a cabinet. And the refrigeration system was installed at the side walls and the exhaust fan was arranged above the cabinet to protect the battery module at high temperature. The results showed that the battery module can be maintained within an appropriate temperature range. But situation of battery module being charging or discharging was not taken into account. As the cooling system was complex and should be continuous working at hot environment, the fixed investment and power consumption may be the obstacle in popularizing.

In order to decrease initial investment and later maintenance, it is necessary to improve the simplification, stability and reliability of the system. What's more, lengthening the time of heat preservation for battery temperature after cooling / heating is important.

As the thermoelectric effects in semiconductors can cause temperature gradients when an electrical current is applied, thermoelectric cooler can create a temperature field lower than ambient temperature. The advantage of the thermoelectric cooler is the absence of moving parts when it is used to convert electrical into cooling capacity [12]. The cooling power can be easily adjusted by the size of current. What's more, the operation mode can be changed from refrigeration to heat when the direction of current is changed. It can work for a long time in high performance without extra maintenance. This could be used to simplify the cooling system and improve the system reliability [13]. Therefore, it is regarded as an attractive method for cooling standby battery of outdoor base station.

Liu [14] proposed the design of thermal management system for lithium ion power battery pack. He put the thermoelectric coolers under the battery pack and used the water jacket to cool the hot

side of thermoelectric cooler. The results show that battery thermal management system with thermoelectric cooler can cool the battery in very high ambient temperature. It can also keep a more uniform temperature distribution in the battery pack than common Battery thermal management system (BTMS). That will extend the life of the battery pack and may save the expensive battery equalization system. But it causes the higher temperature difference within a battery.

Ginart [15] proposed a high-efficiency hybrid semi-adiabatic enclosure consisting of forced air, heating plate and thermo-electrical cooling to cool the stationary outdoor lithium-ion energy storage. When the ambient temperature is suitable, it removes the heat with natural convention or forced air. In low temperatures ambient, the enclosure was transformed into a highly adiabatic system by closing the isolated air and the heat exchange was reduced. When the heat generated from the battery module is not enough for the initial conditions, passive heating is available for temperature increase. When the outdoor temperature exceeds the upper range, a thermo-electrical cooling system is implemented. This method can control the temperature of battery at any moment. The stability and dependability of the system was decreased, as the component moved fluently.

As the PCMs has a large latent heat and appropriate phase change temperature, it can store / release large amounts of heat during the melting / solidifying process [16]. The heat generated by the battery can be absorbed by the PCMs located between the cells of battery modules. When the temperature of the cell reaches the PCMs phase change temperature, the further heat will be stored in PCMs as the latent heat and there is not any further increase in temperature. Passive thermal management based on the PCMs delays the temperature rise when the ambient is hot and maintains the battery below ambient during hot days [17]. In addition, the cooling performance of

the PCM system is superior to that of natural convection system especially at a high current rate [18]. It is more cost-effective and reliable, as it eliminates the need for active cooling/heating during the majority of operating time [19]. Paraffin is the most widely used phase change material due to its high latent heat of phase change and its phase change temperature located in the working temperature arrangement of battery [20-21]. Wang [22] used the composite paraffin and fin structure to cool the cylindrical battery. The results of experiment indicated that the effect of PCMs on improving the uniformity of temperature distribution and restraining temperature rising was obvious. Yan [23] combined the insulation panel and PCMs to make the composite board used in the BTMS. The composite board could effectively improve the heat dissipation capability and temperature uniformity, meanwhile it enhanced the heat-insulation capability of the battery pack to prevent the thermal runaway propagation. Cosentino [24] used the PCMs jacket full of Calcium Chloride to maintain the battery temperature close to or at optimum levels. He pointed out that the average temperature for a 24 hour period must be less than the phase change temperature for the jacket to work properly. Results presented analytical / numerica1calculations of the PCMs Jacket's thermal performance and experimental results obtained from in house and field testing. The results indicated that the jacket was effective in maintaining optimal temperature. The battery jacket is a passive approach to minimize the effects of peak heat loads in the day. The advantage of PCMs is that during its phase change cycle, the temperature of the PCMs stays constant until the phase transition process is complete. The PCMs material in the battery pack can delay the temperature rising and keep the battery module at a more uniform temperature during a day / night cycle. The passive PCMs was also used with other active methods to make coupled battery thermal management. Wu [25] designed a heat pipe-assisted PCMs based BTMS to fulfill the

comprehensive energy utilization for electric vehicles and hybrid electric vehicles. The experimental results showed that the temperature non-uniformity of battery module can be influenced by heat pipes when they are activated under high discharge rates of the batteries. What's more, with forced air convection, the highest temperature could be controlled below 50 ℃ even under the highest discharge rate of 5C and a more stable and lower temperature fluctuation is obtained under cycling conditions. Rao [26] combined the PCMs with mini-channel to cool the battery module. The simulated result indicated that the coupled BTMS presented more effective thermal performance.

In conclusion, semiconductor thermoelectric devices can cool and heat the battery pack in short time and the PCMs can keep the battery temperature in optimum temperature range with the phase change latent heat and acquire uniform temperature distribution during heat preservation process. Considering the standby battery pack of outdoor base stations may operates at long-time low temperature in winter or high temperature in summer, we combined the semiconductor thermoelectric devices and PCMs to control the temperature of standby battery pack for base station. The study focuses on the investigation of the heat preservation performance of this thermal management method for the battery pack in different environment temperature and operating conditions. The effect of arrangement and cooling / heating power for semiconductor thermoelectric devices on the thermal performance in different temperature ambient was investigated in this paper, as well as the time of heat preservation and the power consumption. The temperature range of the thermal management during the cooling and heating process was optimized. And the heat preservation effect of battery pack was studied when the pack discharged or charged in hot environment. At last the performance of pack in continuous cooling and heat

preservation cycle was simulated to study the stability of this thermal management method.

2. Model

2.1 Physical problem

According to the operating characteristic of standby battery for outdoor base station, the battery pack should be kept in comfortable temperature range for a long term. The latent heat of the PCMs is used to withstand the environment and keep the battery at the optimum operating temperature. The semiconductor thermoelectric devices are installed on the surface of battery pack. They could cool / heat the PCMs to recover the heat preservation ability. In the high temperature environment, the semiconductor thermoelectric devices works as cooler until the temperature of monitoring points on the battery reaches prescribed minimum. Because of the naturally convection between pack surface and the environment, the temperature of battery pack increases gradually. And this heat preservation process is lengthened by the phase change latent heat of PCMs. When the temperature of monitoring points reaches the upper limit temperature, the semiconductor thermoelectric devices enters cooling state again. In the low temperature ambient, the current direction of semiconductor thermoelectric devices is changed. The semiconductor thermoelectric devices works as the heater to raise the temperature of battery pack to upper limit.

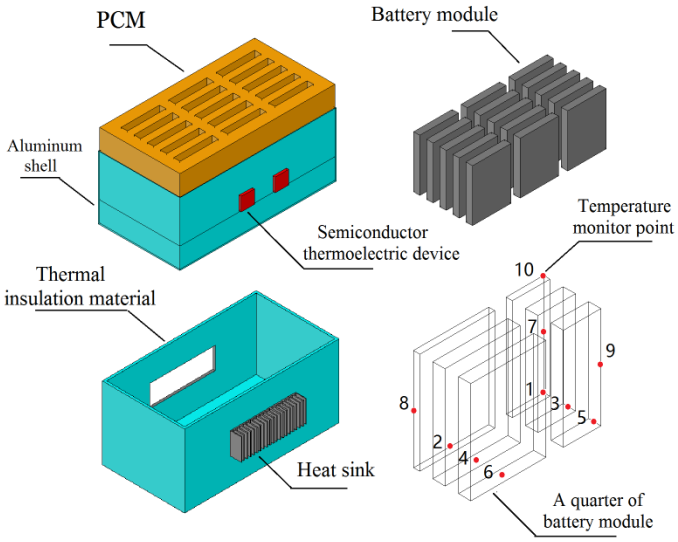

Fig. 1 Schematic of the battery pack with semiconductor thermoelectric devices and PCMs

The schematic of the battery pack was shown clearly in Fig. 1. The 48V and 80Ah battery pack consisted of 60 batteries which were 4 in parallel and then 15 in series. The PCMs filled into aluminum shell was arranged below and around the battery module to stabilize the temperature field of battery. As the operational temperature for lithium-ion battery ranges from 293K to 313K, the PCMs used in the management was n-octadecane, whose phase change temperature T_{PCM} was 301K. The aluminum shell could strengthen the heat transfer among PCMs and improve the uniformity of temperature field, as well as support the battery module. Above the battery module, there was an interspace 4cm in height which was used to arrange the wire. The polyether polyurethane foam was selected as thermal insulation material and covered the battery pack to decrease the natural-convection heat transfer. One side of the semiconductor thermoelectric device was pasted on the surface of aluminum shell. On the other side the heat transfer was strengthened by aluminum fin heat sink. The distribution of 10 monitoring points was shown in the figure and the monitoring points were on the center of the corresponding surfaces. The physical sizes and thermal properties of the battery, PCMs, aluminum, semiconductor thermoelectric device used in

this paper were summarized in Table 1. As the model was symmetrical, only 1/4 part of the module was simulated in this paper to shorten the simulation time.

Table 1 Physical sizes and parameters used in simulation

Nomenclature	Parameters	Value	Source
Size of battery	(mm)	230×170×7	Measured
Size of battery pack	(mm)	710×340×380	Measured
Size of hot end /cold end	(mm)	40×40×1.1	[14]
Size of PN bulk	(mm)	40×40×2.5	[14]
Thermal insulation material thickness	(mm)	10	Measured
Aluminum shell thickness	(mm)	1	Measured
Latent heat of PCMs	L_{PCM} (J/(kg K))	244,000	[16]
Specific heat of battery	c_{pb} (J/(kg K))	2,138	Measured
Specific heat of thermal insulation material	c_{pin} (J/(kg K))	500	[27]
Specific heat of PCMs	c_{pPCM} (J/(kg K))	1,900	[16]
Specific heat of aluminum	c_{pAl} (J/(kg K))	871	[7]
Specific heat of air	c_{pair} (J/(kg K))	1006.43	[7]
Specific heat of hot end /cold end	$c_{phot/cold}$ (kg/m)	419	[12]
Specific heat hot PN bulk	c_{pPN} (kg/m)	200	[12]
Thermal conductivity of battery in X-direction	$\lambda_{b\text{-}X}$ (W/(m K))	0.14	Measured
Thermal conductivity of battery in Y/ Z-direction	$\lambda_{b\text{-}Y/Z}$ (W/(m K))	8.2	Measured
Thermal conductivity of hot end /cold end	$\lambda_{phot/cold}$ (kg/m)	18.5	[12]
Thermal conductivity hot PN bulk	λ_{pPN} (kg/m)	2	[12]
Thermal conductivity of PCMs	λ_{PCM} (W/(m K))	0.21	[16]
Thermal conductivity of aluminum	λ_{Al} (W/(m K))	202.4	[7]
Thermal conductivity of air	λ_{air} (W/(m K))	0.0242	[7]
Thermal conductivity of thermal insulation material	λ_{in} (W/(m K))	0.035	[27]
Ambient temperature	T_{∞} (K)	-	
Gravitational acceleration	g (m/s^2)	9.8	
Density of PCMs	ρ_{PCM} (kg/m)	778	[16]
Density of thermal insulation material	ρ_{in} (kg/m)	70	[27]
Density of aluminum	ρ_{Al} (kg/m)	2719	[7]
Density of battery	ρ_{b} (kg/m)	1991	Measured
Density of air	ρ_{air} (kg/m)	1.255	[7]
Density of hot end /cold end	$\rho_{hot/cold}$ (kg/m)	2900	[12]
Density of hot PN bulk	ρ_{PN} (kg/m)	10922	[12]
Viscosity of PCMs	υ_{PCM} (kg/(m s))	0.01	[16]
Viscosity of air	υ_{air} (kg/(m s))	1.225	[7]
Phase change temperature of PCMs	T_{PCM} (K)	301	[16]
Seebeck coefficients of the P-type	a_p (V/ K)	0.00015	[12]
Seebeck coefficients of the N-type elements	a_n (V / K)	-0.00019	[12]

Resistance of the semiconductor thermoelectric device	$R_s(\Omega)$	2	[14]
Stefan-Boltzmann constant	σ (W /(m^2 K^4))	5.67×10^{-8}	[28]

Gambit was used to mesh the model and FLUENT 17 was used as the simulation software. The independent test of grid number was performed to guarantee accuracy, as shown in Fig.2 (a). And the mesh with 896199 grids was used in the simulation. As the heat transfer process of battery pack in cooling/heating process and heat preservation process was different, the independent test of time step in the two processes were also performed. Considering the cost of calculation, the step of 1 s and 10 s was chosen for the cooling/heating process and heat preservation process in this paper, respectively, as shown in Fig.2 (b) and Fig.2 (c). The convergence criteria for this study were chosen to be 10^{-4} and 10^{-6} for flow and energy, respectively. The theoretical model is developed based on the following assumptions:

(1) The properties of the PCM were constant and equal during the phase change process.

(2) The heat was assumed to be well transferred between fin and ambient.

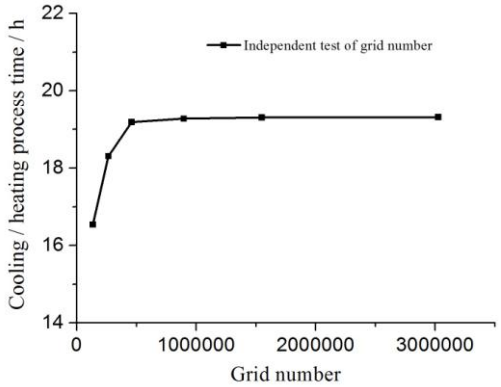

(a)

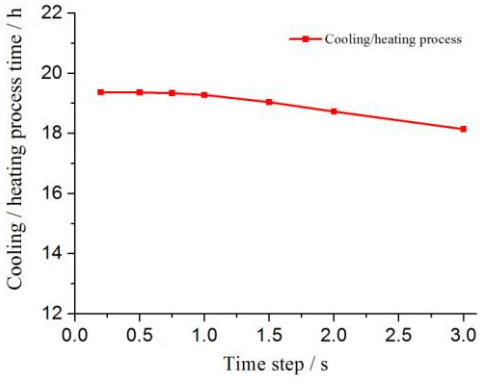

(b)

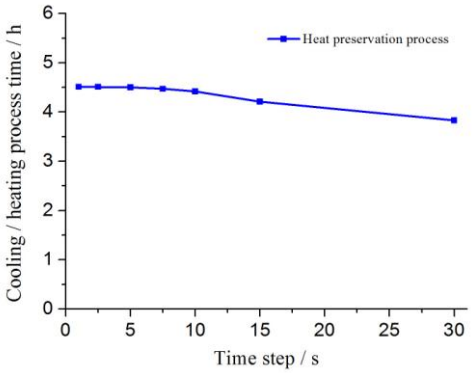

(c)

Fig. 2 Independent test of grid number (a), time step for cooling/heating process (b) and time step for heat preservation process (c)

2.2 Governing equations

As the ambient temperature varies periodic from day to night, it could be described as sinusoidal function: $T_\infty = 313+5\bullet sin(2\bullet t/3600/24-9/12)$. It meant that the daily average temperature was 313K, the ambient minimum temperature and maximum temperature appeared at 3am and 3pm respectively, and the temperature difference of day and night was 10K.

The energy balance equation of the battery, PCMs, semiconductor thermoelectric device and ambient as:

$$q_b + q_s + q_{PCM} + q_{dis-1} + q_{dis-2} = 0 \quad (1)$$

where q_b is the heat generated by the battery, q_s is the heat generated by the semiconductor thermoelectric device, q_{PCM} is the heat absorbed by the PCMs, q_{dis-1} is the heat exchange between out surface of battery pack and ambient, q_{dis-2} is the heat removed by the semiconductor thermoelectric device.

2.2.1. Thermal model of the battery

In order to maintain a 100% charge state, the battery pack was floating charged at all time. And the current of floating charge was always 0.001C and the voltage of floating charge equaled to the open circuit voltage of battery pack. As the SOC (state of charge) of battery maintain in 100%, the heat generated in the floating charge equaled to the electrical energy. And it was calculated as:

$$q_b = I_f U_f \tag{2}$$

where I_f is the current of floating charge, U_f is the voltage of floating charge.

When the battery operated in working condition, the heat generation q_b of the Li-ion battery can be divided into three parts, reaction heat q_r, polarization heat q_p and joule heat q_j, namely [29-32]:

$$q_b = q_r + q_p + q_j \tag{3}$$

The reaction heat q_r is due to electrochemical reactions, which can be obtained as follows:.

$$q_r = -IT_b \frac{dE_{oc}}{dT_b} \tag{4}$$

where I is discharge current. E_{oc} and T_b are the open-circuit voltage and temperature of battery, respectively. And the dE_{oc}/dT_b is a function of density, SOC (state of charge) and battery temperature, which can be got from reference [27].

The resistance of battery is called ohmic resistance R_o when the current is zero. During the discharging process of battery, the current flows through the battery and battery voltage is larger than open circuit potential as the electrode potential deviates from balance potential. The difference between battery voltage and open-circuit potential can be expressed as IR_p , where R_p stands for the polarization resistance. The energy loss by polarization dissipated as heat q_p.

Therefore, polarization heat q_p can be expressed by:

$$q_p = I^2 R_p = I^2 (R_{total} - R_o) \tag{5}$$

where R_{total} represents total resistance. R_{total} is the real resistance during the battery's discharge process. Meanwhile, joule heat q_j generated by current flows through resistance is as follow:

$$q_j = I^2 R_o \tag{6}$$

The heat generation q_b within the Li-ion battery during discharge can be expressed as:

$$q_b = I^2 R_t - I T_b \frac{dE_{oc}}{dT_b} \tag{7}$$

The energy conservation equation of battery can be expressed as:

$$\frac{\partial}{\partial t}(\rho_b c_{pb} T_b) = \lambda_b \nabla^2 T_b + q_b \tag{8}$$

Where ρ_b, c_{pb} and λ_b are the density, heat capacity and thermal conductivity of battery, Similarly, the energy conservation equation of PCM is:

$$\frac{\partial}{\partial t}(\rho_{PCM} c_{pPCM} T_{PCM}) + q_{PCM} = \lambda_{PCM} \nabla^2 T_{PCM} \tag{9}$$

Where ρ_{PCM}, c_{pPCM} and λ_{PCM} are the density, heat capacity and thermal conductivity of battery, respectively. The q_{PCM} is the heat absorbed by the PCM during the phase change process. During the meling process, the q_{PCM} is the arithmetic product of liquid phase volume fraction and phase change enthalpy. During the solidification process, the q_{PCM} is the arithmetic product of solid phase volume fraction and phase change enthalpy.

2.2.2. Thermal model of the semiconductor thermoelectric device

Similar to [12] the semiconductor thermoelectric device is modeled by three parts: cold end, hot end, and PN bulk. The cold end that included a ceramic plate is adhered to the aluminum shell. The hot end that included a ceramic plate is cooled by the fin to keep a stable temperature. The PN bulk has the same area as the ceramic plate, so the thermal parameters would change accordingly.

The general equations of the thermal models of the three parts are the same as the battery. Only the heat generation term q in (8) is treated differently, shown as follows.

for cold end,

$$q_{cold} = \frac{I_s(\alpha_P - \alpha_N)T_{cold}}{V_{cold}} \tag{10}$$

for hot end,

$$q_{hot} = \frac{I_s(\alpha_N - \alpha_P)T_{hot}}{V_{hot}} \tag{11}$$

for PN bulk,

$$q_{PN} = \frac{I_s{}^2 R}{V_{PN}} \tag{12}$$

where I_s is the current supplied to the semiconductor thermoelectric device, R is the resistance of the semiconductor thermoelectric device, a_P and a_N are the Seebeck coefficients of the P-type and N-type elements, $T_{??old}$ and T_{hot} are the temperature of cold end and hot end, respectively, and $V_{??old}$, V_{PN}, and V_{hot} are the volume of the three parts.

During the cooling/heating process the q_s is equal to the q_N. When the battery pack is cooled by semiconductor thermoelectric device, the $q_{dis\text{-}2}$ is equal to q_{cold}. When the battery pack is heated, the $q_{dis\text{-}2}$ is equal to q_{hot}.

Radiation is significant for most systems interchange heat with the ambient and the radiation analysis should accompany a natural convection analysis especially in high temperature ambient [33]. The boundary equations in each direction can be expressed as follows:

$$-\lambda_{in}\frac{\partial T}{\partial x}=h(t_{out}-T_{\infty})+\varepsilon\sigma(t_{out}^{4}-T_{\infty}^{4}),\quad x=0,X \tag{13}$$

$$-\lambda_{in}\frac{\partial T}{\partial y}=h(t_{out}-T_{\infty})+\varepsilon\sigma(t_{out}^{4}-T_{\infty}^{4}),\quad y=0,Y \tag{14}$$

$$-\lambda_{in}\frac{\partial T}{\partial z}=h(t_{out}-T_{\infty})+\varepsilon\sigma(t_{out}^{4}-T_{\infty}^{4}),\quad z=0,Z \tag{15}$$

where λ_{in} means the heat conductivity coefficient of thermal insulation material, h denotes the convection heat-transfer coefficient at the battery surface, T_{∞} is the ambient temperature, t_{out} is the out surface temperature of battery pack, ε and σ are the battery surface emissivity and the Stefan-Boltzmann constant, respectively. And ε is a dimensionless quantity between 0 and 1 [29]. It represents the fraction of blackbody radiation that the surface in question emits (a black body by definition has ε= 1).

Here, using empirical correlation to determine h :

$$Nu_{m}=C(GrPr)_{m}^{n} \tag{16}$$

$$Gr=\frac{g\beta_{V}\Delta Tl^{2}}{\upsilon u}\frac{ul}{\upsilon}=\frac{g\beta_{V}\Delta Tl^{3}}{\upsilon_{2}} \tag{17}$$

$$h=Nu\frac{\lambda_{air}}{l} \tag{18}$$

where Nu_{m} is the Nusselt number calculated as mean temperature, the qualitative temperature t_{m} equal the mean temperature of ambient temperature T_{∞} and out surface temperature of battery pack t_{out}, Gr is the Grashof number, Pr is the Prandtl number, ΔT is the temperature difference of t_{∞} and t_{out}. For the air fits the character of ideal gas, the coefficient of cubical expansion β_{V} in Gr

equals to 1/*T*. And the value of *T* can use the mean temperature of boundary layer. The *l* is characteristic length, *g* is gravitational acceleration, *u* is the flow velocity of air, υ is kinematic coefficient of viscosity and the λ_{air} is the heat conductivity coefficient of air. When the *h* on the 4 flanks of battery pack is calculated , *C* and *n* in Eq. (16) are constant [34].

3 Results and discussion

The effect of arrangement and power of the semiconductor thermoelectric devices on the performance of thermal management were investigated. The upper limit and lower limit of the temperature for thermal management and location of thermocouple were confirmed. The performance of thermal management was depicted by cooling / heating time, heat preservation time, power consumption and ΔT_{max} which represented temperature uniformity. And the availability of temperature restraining in different changing / discharging process and different ambient temperature was simulated to study the adaptability to different working conditions. At last the 5 continuous cooling / heat preservation cycles were used to research the stability of the standby battery pack for outdoor base station.

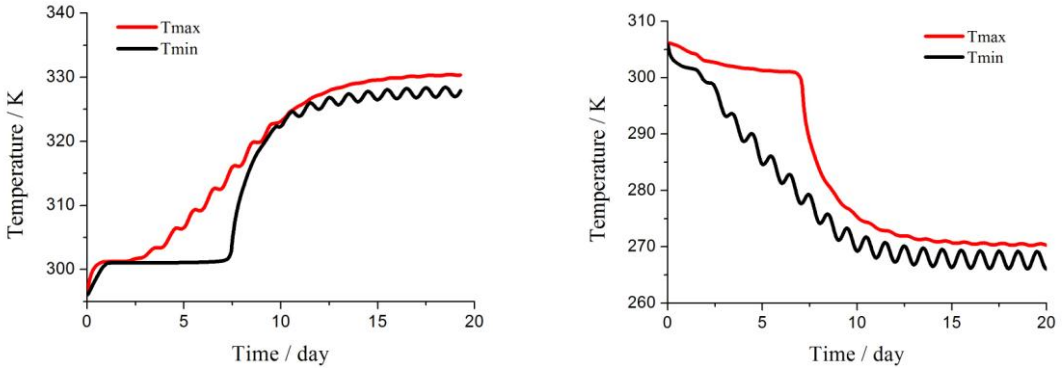

Fig.3. Temperature of battery module with passive cooling versus time with different environment temperature, (a) average ambient temperature was 323K, (b) average ambient temperature was 263K

The variation of battery temperature in the pack with passive thermal management based on

PCMs was shown in Fig.3. When the average ambient temperature was higher than the T_{PCM} of PCMs, the battery temperature increased over time. During the temperature rising, the maximum temperature (T_{max}) stayed at the 301K for about 2 days, when the PCMs around T_{max} point was melting and absorbing much heat. After a full meltdown, the ability of restraining battery temperature rising with latent heat was exhausted. The battery temperature rose continuously. T_{max} of battery module reached 313K after 7 days because of the high ambient temperature and heat generated in floating charge. And T_{max} remained at 330K after 15 days. In the cold ambient, the temperature of battery decreased over time and reached 270K after 10 days, as the heat generated in floating charge was less than the heat exchange between battery pack and ambient.

The PCMs in the battery pack delayed the battery temperature reaching ambient temperature as the PCMs absorbed or released large numbers of heat. After the PCMs completing phase change, the ability was weakened. In order to recover the ability of heat preservation before the battery temperature out of optimum range, it was necessary to cool the PCMs to solid state in hot ambient or heat the PCMs to liquid state in cold ambient. So, the semiconductor thermoelectric devices were used to cool and heat the PCMs before the battery temperature reaching the upper and lower limit, respectively. And the upper and lower limit of battery temperature was set as 296K ~ 308K provisionally.

3.1 The effect of arrangement of semiconductor thermoelectric device

In order to research the effect of arrangement of semiconductor thermoelectric device on the time of cooling / heating process, heat preservation process and the uniformity of the battery temperature field, we simulated the thermal performance of battery module with four different

arrangement of semiconductor thermoelectric devices. As the space in battery pack was limited, the pack was installed 4 semiconductor thermoelectric devices. The schematic diagram of semiconductor thermoelectric devices arrangement in different cases was shown in Fig.4. In the case 1, semiconductor thermoelectric devices were under the battery module and distributed uniformly. In the case 2 and 3, semiconductor thermoelectric devices were installed at the two opposite sides of the battery module. In case 4, semiconductor thermoelectric devices distributed at four flanks of the pack. During the simulation, the temperature of ten points of the battery module was monitored, as well as $T_{\max}$ and T_{min} of the battery module. The location of the monitoring points was shown in Fig.1.

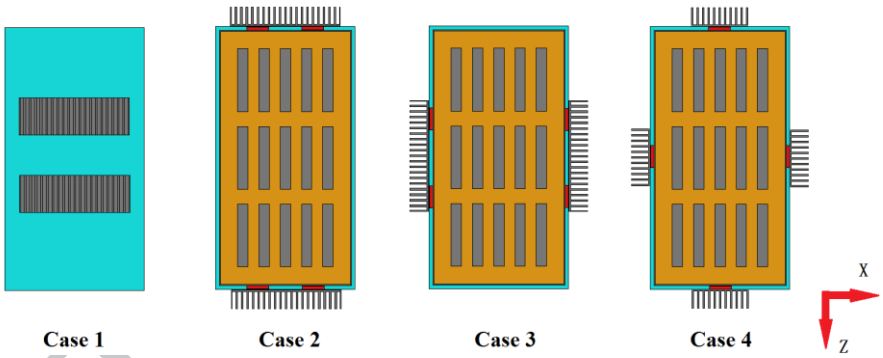

Fig.4 Arrangement of the semiconductor thermoelectric devices

3.1.1 Cooling and heat preservation in high temperature ambient

If $T_{\max}$ of battery module reached 308K in high temperature ambient, the semiconductor thermoelectric devices started to work as a cooler. In the cooling process, the liquid state PCMs in the battery pack was cooled by the thermoelectric coolers until T_{min} of battery module reached 296K. After the cooling process, the majority of PCMs in the battery pack was solid state, as the Table 2 showed, and could maintain the temperature of battery module in the high temperature ambient by absorbing the heat with phase change latent heat. After $T_{\max}$ of battery module rising to

308K with natural-convection heat transfer, the semiconductor thermoelectric devices cooled the PCMs once again to recover the ability of keeping battery cool. In the simulation, the average temperature of the ambient was 323K and the total cooling power of the 4 semiconductor thermoelectric devices was 200W. The initial temperature of each part in the pack was 308K. The Fig.5 showed the temperature variation of monitoring points and ΔT_{max} of the battery in the cooling and heat preservation process with different semiconductor thermoelectric devices arrangement.

As the cooling time increased, the temperature of each monitoring points decreased gradually and ΔT_{max} of the battery module presented a rising trend in general. At the end of cooling process the ΔT_{max} of the battery module was largest. The time of cooling process for case 3 was longest and the cooling time of case 2 was shortest.

In the case 1, the temperature of monitoring points closed to the thermoelectric coolers in the Y direction was lower than others. At the earlier stage of cooling process, the descent velocity of monitoring points temperature increased gradually. When T_{min} of the battery module declined to 301K the descent velocity decreased. In the case 2, the heat in the battery pack was absorbed by the thermoelectric coolers along the Z direction. In this direction the sizes was largest and the thermal resistance was largest. And the temperature gradient in Z direction was enlarged. As a result the temperature difference of battery module in case 2 higher compared than others during the whole cooling process. In the case 3, before T_{min} of the battery module reaching 301K, the temperature difference was small. At the later period of cooling process the temperature of ten monitoring points divided into three groups. These monitoring points distributed on the three rows of batteries. And the PCMs between the batteries increased the thermal resistance. In the case 4,

the semiconductor thermoelectric devices surrounded the battery module and distributed more uniformly. But the cooling performance of case 4 was weakened because of the poor heat transfer in Z direction. The temperature variation fell in between the temperature variation of case 1 and case 3.

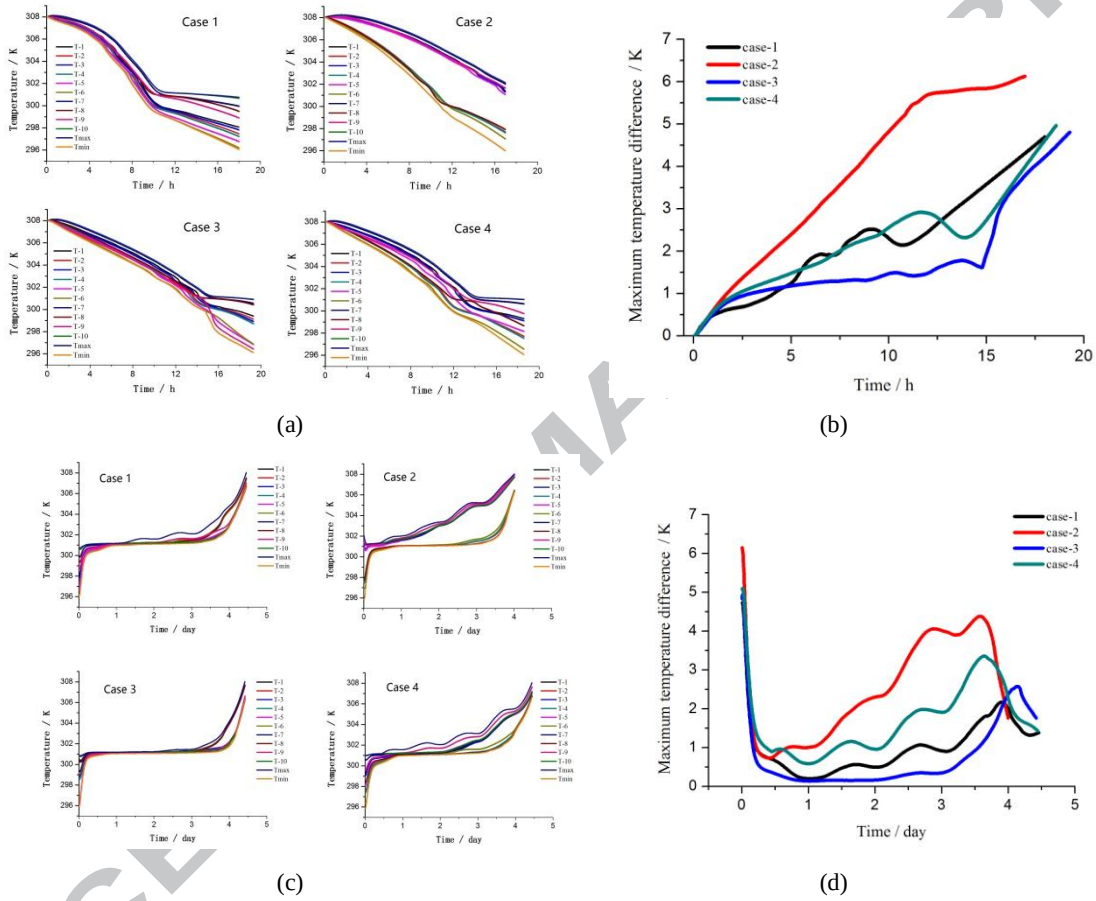

Fig.5 (a)Temperature of monitoring points, (b) ΔT_{max} of the battery versus time in cooling process, (c) temperature of monitoring points, (d) ΔT_{max} of the battery versus time in heat preservation process in high temperature ambient

Table 2 Volume fraction of solid state PCMs after cooling process

case	1	2	3	4
Volume fraction (%)	71.4	64.62	73.98	72.02

After cooling process the majority of PCMs in the battery pack was cooled to solid state and recovered the ability of restraining battery temperature with latent heat. The volume fraction of solid state PCMs after cooling process in different cases was showed in Table 2. More PCMs was

cooled in the case 3 compared with that in other cases. As the Fig.5(c) showed, the difference of heat preservation time in different cases was small. The time of cooling process in case 1, 3 and 4 was similar as the volume fraction of solid state PCMs in these cases was similar. The time of heat preservation time was influenced heavily by the volume fraction of solid state PCMs. Comparing the Fig.5(a) and Fig.5(c), it is clear that the case with more uniform temperature field in the cooling process had more uniform temperature field in the heat preservation. In the preliminary stage of heat preservation process, the temperature rising and temperature gradient decreasing in short time mainly resulted from the stopping of thermoelectric coolers and the heat generated in floating charge of battery module. In the middle period of heat preservation process, the solid state PCMs began to melt and absorbed the heat from the ambient and battery module. In case 3, the battery temperature rose slowly and the temperature difference of battery module was less than 1K. While, T_{max} of battery module in case 2 and 4 increased gradually in middle period. It resulted from the non-uniform temperature field of PCMs caused by the cooling process. The PCMs far from the thermoelectric cooler was not cooled efficiently and was still liquid state at the end of cooling process. In the heat preservation process, the battery temperature rising was not restrained by the PCMs' sensible heat. The temperature of battery close to the melting PCMs remained at 301K. As a result, the battery temperature difference in case 2 and 4 increased continuously. In the later stage of heat preservation process, the majority of PCMs in the battery pack was liquid state. Heat generated by floating charge battery module was absorbed in the form of sensible heat by PCMs. The temperature of battery module presented a fast rising trend and the temperature difference decreased gradually.

3.1.2 Heating and heat preservation in low temperature ambient

When the battery pack was set in low temperature ambient, the battery temperature decreased gradually. After T_{min} of the battery module reaching the lower limit, the current direction of the semiconductor thermoelectric devices was changed and the semiconductor thermoelectric devices started to heat the solid state PCMs until $T_{\max}$ of battery module reached 308K. After the heating process, the majority of PCMs was liquid state and could maintain the temperature of battery module in the low temperature ambient by releasing heat with phase change latent heat. When T_{min} of battery module dropped to 296K, the thermoelectric heaters heat the PCMs once again to recover the ability of keeping battery warm. In the simulation of this part, the average ambient temperature was 263K and the total heating power of the 4 semiconductor thermoelectric devices was 200W. The initial temperature of each part in the pack was 296K. The Fig.6 showed the temperature variation of monitoring points and ΔT_{max} of the battery in the heating and heat preservation process with different semiconductor thermoelectric devices arrangement. The temperature variation presented some similar characters with that in the cooling process, as well as some different characteristics.

There were some similar characteristics as the Fig. 6 showed. During the process of the semiconductor thermoelectric devices working, the temperature of each monitoring points departed from the ambient temperature over time gradually. The temperature of monitoring points closed to the semiconductor thermoelectric devices changed faster than others. And ΔT_{max} of the battery module presented a rising trend in general. In the heat preservation process, the temperature difference declined in short time as the temperature gradient caused by thermoelectric heaters was decreased by heat transfer. Then it rose slowly with fluctuations over time. The temperature of monitoring points closed to air changed faster than others because of the low heat

capacity of air and the low temperature ambient. And ΔT_{max} of the battery module appeared at the end of heating process. The volume fraction of liquid state PCMs after heating process was shown in Table 3. And it influenced the time of heat preservation. The time of heating process and heat preservation process in case 3 was longest in all the 4 cases. In majority of the process, the battery temperature difference in case 3 was lower than others. And the time of heating process and heat preservation process in case 2 was shortest. The big thermal resistance in Z direction weakened the heat transfer and reduced the uniformity of temperature field. The temperature of above surface of battery module decreased with fluctuations, as it was influenced greatly by the ambient temperature. The temperature difference of battery module rose with fluctuations.

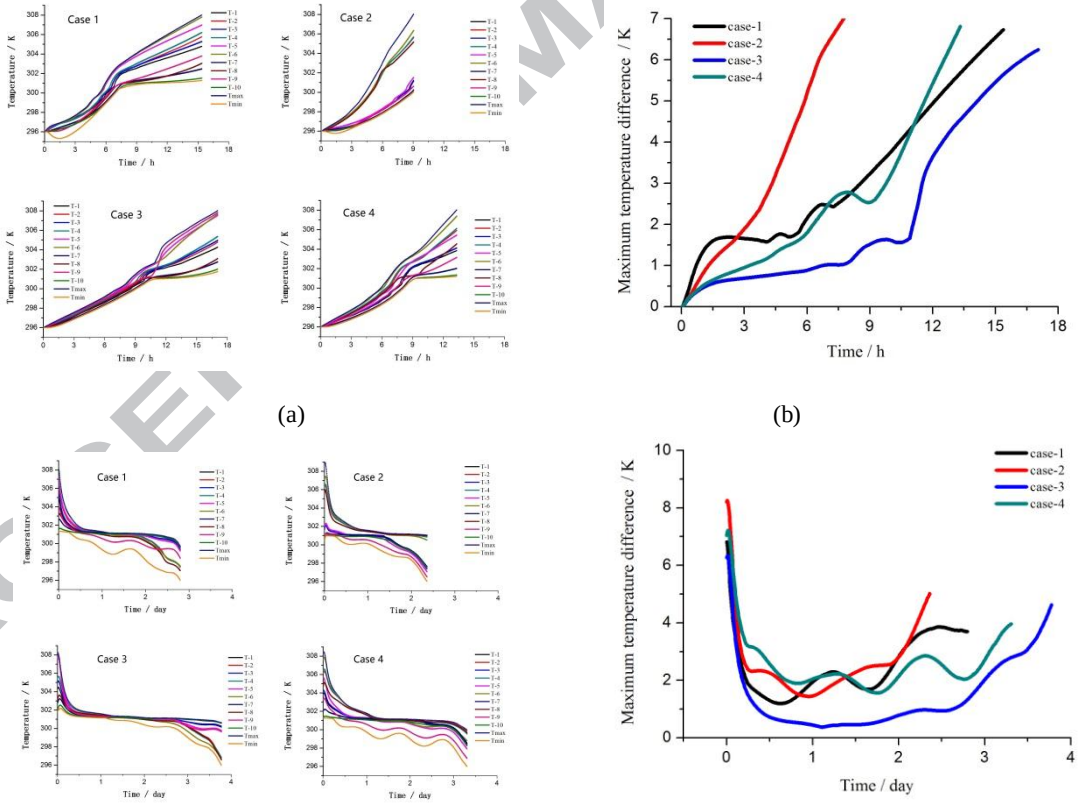

Fig.6 (a)Temperature of monitoring points, (b) ΔT_{max} of the battery versus time in heating process, (c) temperature of monitoring points, (d) ΔT_{max} of the battery versus time in heat preservation process in high temperature ambient

Table 3 Volume fraction of liquid state PCMs after heating process

case	1	2	3	4
Volume fraction (%)	69.15	63.95	83.2	73.73

The particular characteristics of heating and heat preservation in cold ambient were also shown in the Fig.5. At the end of heating process, ΔT_{max} of the battery module in different cases was close. In the later stage of heat preservation process, ΔT_{max} of battery module did not decrease as it presented in hot ambient. The time of heat preservation in low temperature ambient was shorter than that in hot ambient. The difference between T_{PCM} of PCMs and the ambient temperature increased. As a result, the difference of heat preservation time in different cases was enlarged in cold ambient.

In this part, the effect of arrangement of semiconductor thermoelectric devices on the effect of battery thermal management both in high and low temperature ambient was investigated. Considering the time of semiconductor thermoelectric devices working process and heat preservation process, as well as ΔT_{max} of battery module in each process, the arrangement of semiconductor thermoelectric devices in case 3 was best.

3.2 The optimizing of temperature range

In general, it was considered benefit to prolong the battery service life when ΔT_{max} of the battery module is smaller than 5K. The result in section 3.1 showed that the temperature difference of the battery module in each process was influenced by the T_{PCM} and the upper / lower limit of battery temperature.

At the ending of cooling process, when T_{min} of the battery reached 296K, $T_{\max}$ was 301K. Because the heat conductivity coefficient of the PCMs was lower than the cell and the aluminum. At the end of cooling process, the PCMs far from the semiconductor thermoelectric devices was

solidifying. So the temperature of the battery part near solidifying PCMs was 301K. For the same reason, during the heating process T_{min} still remained at 301K when T_{max} of the battery reached 306K.

So the lower limit temperature should be 296K and the upper limit temperature of the battery module should be 306K. In other words, the upper limit should be 5K higher than the T_{PCM} of PCMs and the lower limit should be 5K lower than the T_{PCM}. And ΔT_{max} during the cooling and heating process can be controlled within 5K. Temperature variation of batter module of case 3 with the temperature range of thermal management between 296K and 306K in different process was shown in the Fig.7. As the temperature range was reduced, the time of cooling and heating process was decreased obviously. But the time of heat preservation changed a little. It indicated that the redundant cooling or heating process exacerbated the non-uniform temperature field. But it was limited to improve the effect of heat preservation. What's more, the reduced temperature range leaded to smaller ΔT_{max}, as the Fig.7 (e) and Fig.7(f) showed. In the majority of cooling/heating process and heat preservation process, ΔT_{max} of battery module was less than 3 K, which was propitious to battery life. The time of ΔT_{max} exceeded 5K after cooling was 0.13 hour. Temperature field of battery module was considered uniform in all the thermal management.

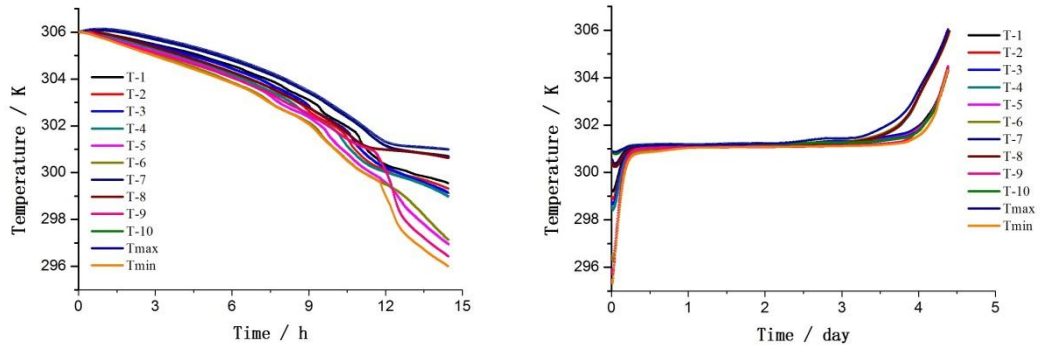

(a) (b)

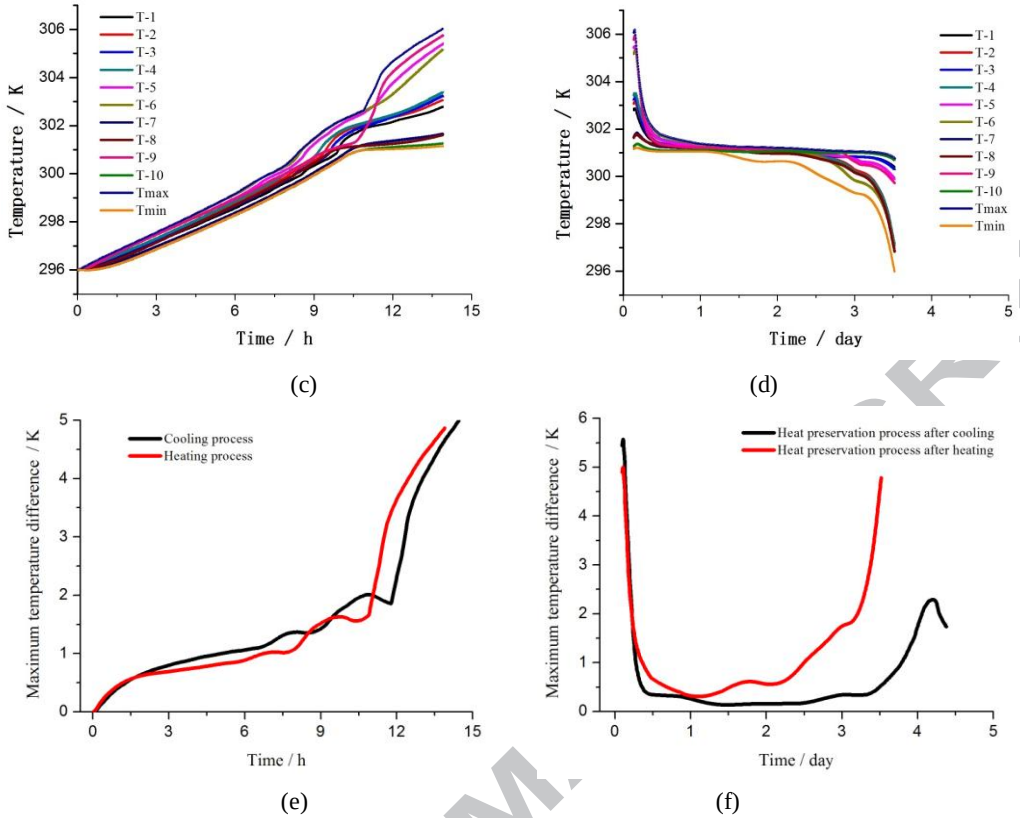

Fig.7 Temperature variation of battery module of case 3 in (a) cooling process, (b) heat preservation process in high temperature ambient, (c) heating process, (d) heat preservation process in low temperature ambient with the temperature range of thermal management between 296K and 306K, (e) ΔT_{max} of battery module in cooling/heating process, (f) ΔT_{max} of battery module in heat preservation process

As the Figure 5(a) showed, in the cooling process the temperature of monitoring point 9 was close to T_{min} of the battery module. And the difference value of them was 0.36K. What's more, in the heating process the difference value of the temperature of monitoring point 9 and $T_{\max}$ of the battery module was 0.21K, as the Figure 6(a) showed. Because the location of point 9 was close to the semiconductor thermoelectric devices and the temperature of point 9 was first and most heavily influenced. So the thermocouple can be set at the location of point 9 to monitor the temperature. And the measured value of the thermocouple can be used as the temperature signal to stop the semiconductor thermoelectric devices.

As the Fig. 5(c) showed, in the heat perseveration process after cooling the temperature of monitoring point 10 was close to $T_{\max}$ of the battery module. And the difference value of them was

0.31K. In the heat perseveration process after heating the difference value of the temperature of monitoring point 10 and T_{min} of the battery module was 0.5K, as the Fig 6(c) showed. That is because the location of point 10 was close to the pack above surface. As the heat capacity of air above the battery module was far below the PCMs and the free convection heat transfer coefficient of pack above surface was bigger than others, the temperature of point 10 was affected by the ambient greatly. What's more, the point 10 is far from the center of battery pack and was affected slightly by the heat generated in the floating charge. So the thermocouple can be set at the location of point 10 to monitor the temperature. And the measured value of the thermocouple can be used as the temperature signal to start the semiconductor thermoelectric devices.

3.3 The effect of cooling and heating power

As the arrangement of semiconductor thermoelectric devices and the temperature range of thermal management were confirmed, the cooling / heating power was another key factor to influence the time of cooling / heating process and heat preservation process, temperature field and power consumption. In this section, the cooling / heating power was set as 100W, 150W, 200W, 250W and 300W to investigate the effect.

The simulation results of semiconductor thermoelectric devices working in high temperature were shown in Fig.8. As the Fig.8 (a) showed, both the time of cooling process and heat preservation process presented a decline trend and the declining slowed down with the cooling power increasing. When the PCMs was cooled by larger cooling power semiconductor thermoelectric devices, the temperature field in the battery pack was more non-uniform and less PCMs in the pack was in solid state decreased at the end of cooling process. As a result the heat

preservation process was shortened. The power consumption in the cooling / heat preservation cycle and the average daily value was shown in Fig.8 (b). The curve of average daily power consumption indicated that increasing cooling power leaded to the power consumption decreasing. But the effect was not obvious. As the cooling power increased, the ΔT_{max} at same stage of cooling process increased. At the middle stage the temperature difference decreased for a short time, when the PCMs close to the battery began to melt. Then the temperature difference rose more quickly. The variation of temperature difference of battery module in heat preservation was similar. When the total cooling power was more than 150W, the temperature difference decreased at the later stage of heat preservation. The smaller cooling power led more solid phase PCMs in the pack. During the heat preservation process the battery temperature kept rising because of the heat generated in floating charge and high temperature ambient. If there was some solid phase PCMs in the battery pack at the later stage of heat preservation process, the temperature of battery pack close to these PCMs was low and the temperature difference of battery rose continuously. When the cooling power was small, the time of battery module ΔT_{max} exceeded 3 K was longer in all the cooling and heat preservation cycle. What's more, the longer cooling process decreased the life span of the semiconductor thermoelectric devices. However, with the increasing cooling power, the heat dissipation load of hot end increased. Therefore, the best choice of cooling power was 200W.

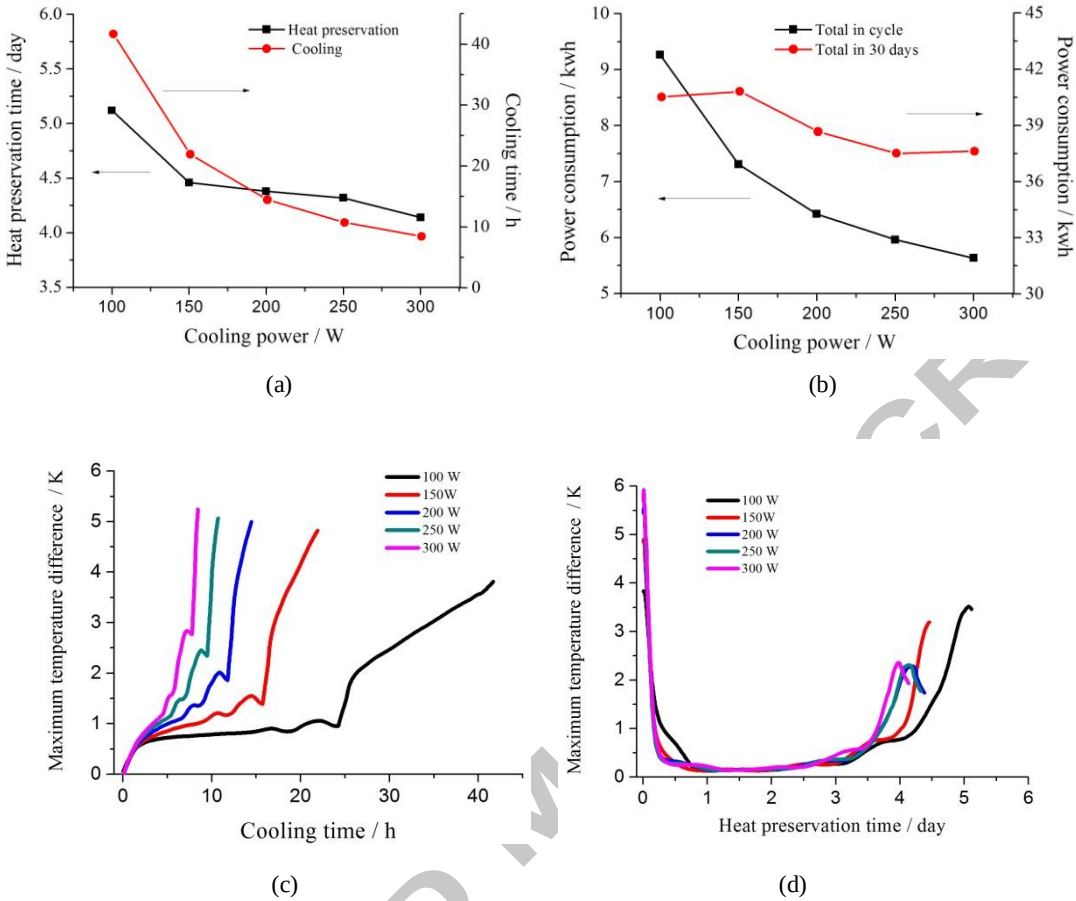

Fig.8 (a) Time of cooling process and heat preservation process, (b) Power consumption, (c) Temperature difference in cooling process, (d) Temperature difference of the battery in high temperature ambient versus different cooling power

The effect of heating power on thermal management in low temperature was shown in Fig.9. The variation trend of heating and heat preservation process time was similar to that in high temperature. The COP (coefficient of performance) of semiconductor thermoelectric devices was higher than 1 when it worked as a heater. So the power consumption of heating process was low. The decline of heat preservation time versus different heating power was more obvious than that in high temperature. Because heat transfer coefficient and temperature difference during the natural convection were enlarged. At the later stage of heat preservation process, ΔT_{max} continued to increase as T_{min} decreased continuously and $T_{\max}$ stayed at 301K. Higher heating power made shorter heating time and heat preservation time. In order to decrease the heating frequency and

consumption, the battery pack heated with 200W was suitable.

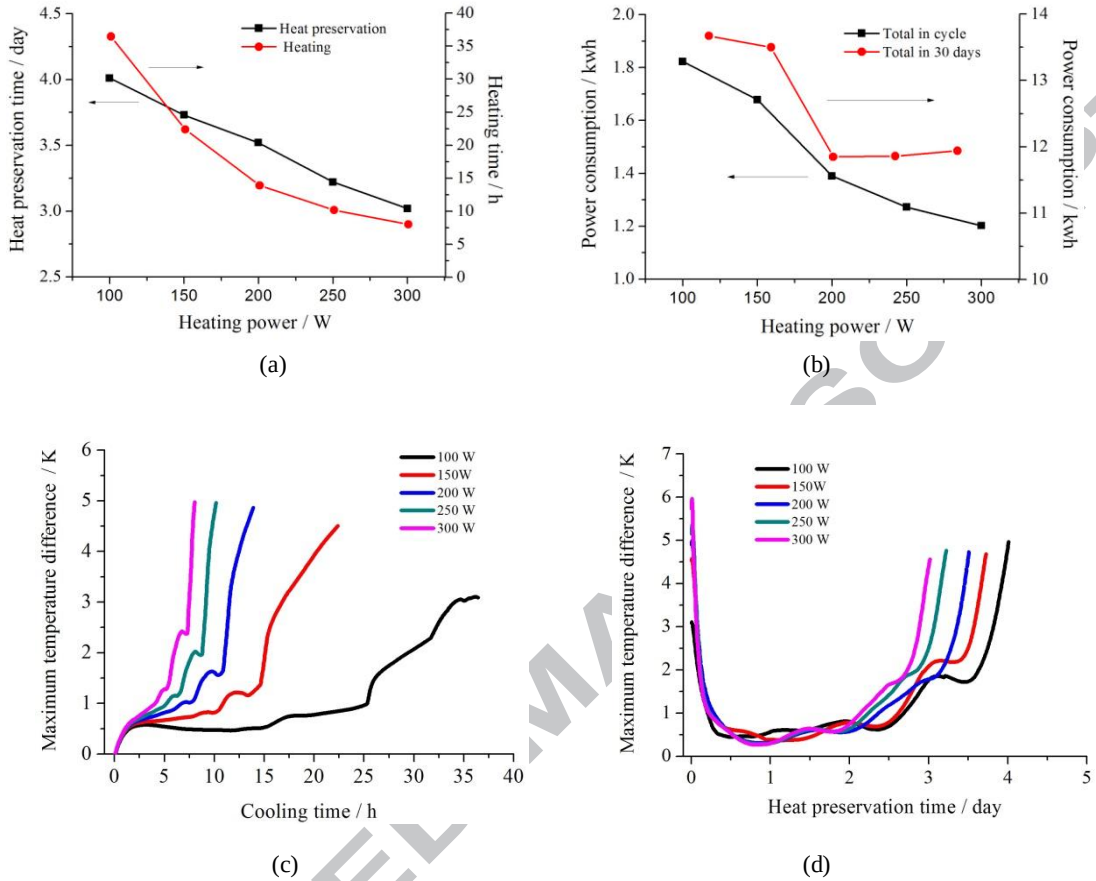

Fig.9 (a) Time of heating process and heat preservation process, (b) Power consumption, (c) Temperature difference in heating process, (d) Temperature difference of the battery in high temperature ambient versus different heating power

3.4 The performance of thermal management in different ambient temperature

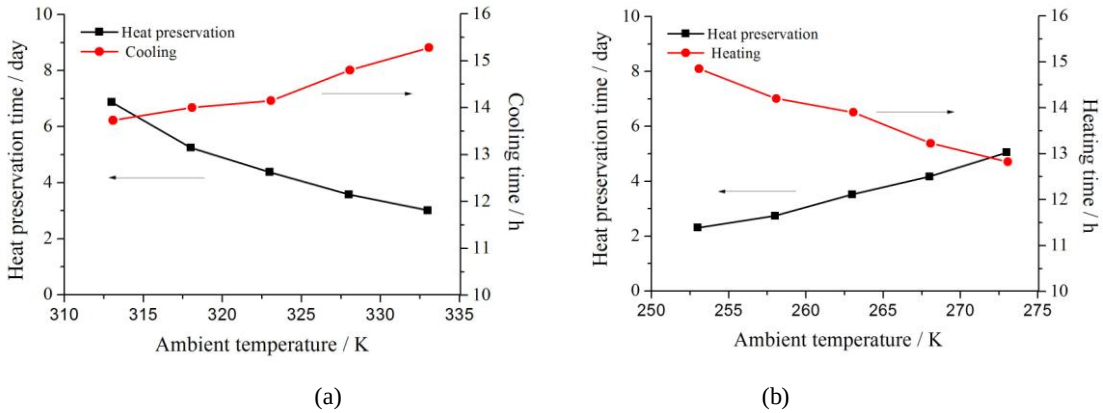

Fig.10 Time of heating process and heat preservation process versus temperature; (a) in high temperature ambient,

(b) in low temperature ambient

The ambient temperature might change heavily over season and geographic location. In order to research the adaptability of battery pack to temperature, the performance of thermal management in temperature range of 253K~273K and 313K~333K was simulated respectively. The semiconductor thermoelectric devices were arranged as case 3 and the total heating power and cooling power were both 200W.

When the ambient temperature was higher than T_{PCM}, the mean temperature difference of natural-convection heat transfer and the coefficient of heat transfer were enlarged, as the ambient temperature increased. The heat absorbed by the battery pack surface increased. It led to the increasing of cooling process time and decreasing of heat preservation time. When the ambient temperature was lower than T_{PCM}, the mean temperature difference of natural-convection heat transfer and the coefficient of heat transfer were decreased, as the ambient temperature increased. The heat dissipation of the battery pack surface was decreased. It led to the decreasing of heating process time and increasing of heat preservation time. As the Fig.10 showed, the working time of semiconductor thermoelectric devices was less than 16 hours and the time of heat preservation process was more than 2 days as the ambient temperature range was between 253K and 333K. It indicated that this thermal management method could keep the battery module in optimum temperature for a long time after a short cooling / heating process.

3.5 The performance of thermal management in discharging and charging process

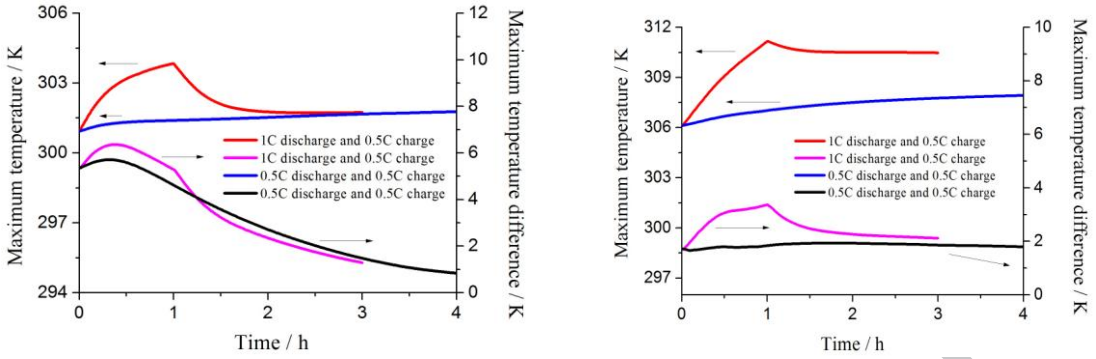

Fig.11 Temperature variation of battery module in discharge-charge process versus time; (a) discharged at the beginning of heat preservation process, (b) discharged at the beginning of cooling process

The standby battery for outdoor base station might be put into operation and discharge at any moment due to the uncertainty of the actual working conditions. In order to investigate the performance of thermal management in different working conditions, we simulated the temperature variation of battery module in 0.5C discharging and charging process, as well as the 1C discharging and 0.5C charging process. As the discharging time was uncertain, we simulated the two most representative working conditions. They were discharged at the beginning of heat preservation process and discharged at the beginning of cooling process. In this simulation, the semiconductor thermoelectric devices were arranged as the Case 3 and the cooling power was 200 W. The temperature variation was shown in Fig.11.

At the beginning of heat preservation process, $T_{\max}$ of battery module was about 301K and ΔT_{max} was about 5K, as the semiconductor thermoelectric cooling and phase change latent heat of PCMs functioned. When the battery pack discharged, both $T_{\max}$ and ΔT_{max} of battery module increased in short time. As the heat generation of battery increased with current increasing, the temperature and temperature difference increased quickly. As the heat was partly absorbed by the PCMs in the form of phase change latent heat, the increasing trend was slowed down. After 1C

discharging the battery was charged with 0.5C. The heat generation was decreased and was lower than the heat absorbing of PCMs. T_{max} decreased gradually and then remained unchanged. In the 0.5C discharging and charging process, the heat generation of battery and heat absorbing of PCMs balanced and T_{max} was steady. The temperature difference result from cooling was decreased gradually due to the heat generation of battery.

At the beginning of cooling process, T_{max} of battery module was 306K and the temperature field was relatively uniform. After the previous heat preservation process, the majority of the PCMs was in liquid state and the phase change latent heat could not function to restrain the temperature rising in discharging process. When the battery discharged with 1C current, T_{max} and ΔT_{max} of battery module increased rapidly. After discharging, the heat generation of 0.5C charging process decreased. The temperature and temperature difference dropped a little and then remain unchanged, as the heat generation was absorbed by the PCMs in the form of sensible heat. In the 0.5C discharging and charging process, the heat generation was unchanged and the temperature of battery module increased slowly and the temperature difference remained unchanged. The results showed that the PCMs in the pack played an important role to restrain the temperature rising effectively in the discharging and charging process. As the semiconductor thermoelectric devices and the battery module were separated by the PCMs, the active cooling performance was not obvious.

As most representative working condition was considered, in the 1C discharging and 0.5C charging process T_{max} of battery module was under the 313K, which did not exceed the optimal temperature range of lithium battery.

3.6 The performance of thermal management in continuous cooling/heating and heat preservation cycle

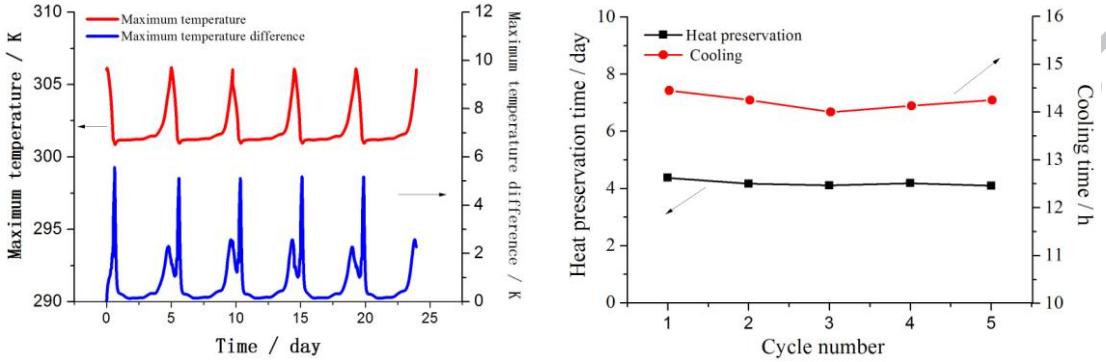

(a) (b)

Fig.12 (a) $T_{\max}$ and ΔT_{max} of battery module, (b) time of cooling process and heat preservation process during continuous cooling and heat preservation cycle

The Fig.12 showed the temperature variation of battery module and time of different process in the continuous cooling and heat preservation cycle, as the average ambient temperature was 323K. It indicated that in the continuous process $T_{\max}$ and $\Delta T_{\max}$ of the battery module changed periodically. The time of first cooling and heat preservation was longer, as the initial temperature field was uniform in the beginning of first cooling process. After that the time of subsequent cooling process floated around 14 hours. And the time of subsequent heat preservation process floated around 4 days and the changing of cooling process was bigger. As the ambient temperature fluctuated in a 24-hour cycle and the cooling time was less than 15 hours, the cooling process began at different time would bear different ambient temperature. The heat transfer on the pack surface was different and it led the different cooling time. While, the heat preservation time was about 4 days and was less affected by the ambient temperature fluctuation but was influenced heavily by the cooling time. In a similar way, the battery pack would show the similar characters during the continuous heating and heat preservation process in the low temperature ambient.

The results showed that the standby battery pack with semiconductor thermoelectric device and

PCMs still had stable time of cooling and heat preservation process in different temperature ambient. The heat preservation effect did not fail and was beneficial to prolong the battery life.

4 Conclusion

This paper presented the thermal management of 48V 80Ah Lithium-ion battery packs for base station at different temperature based on the semiconductor thermoelectric device and phase change materials. The study focuses on the heat preservation effect of semiconductor thermoelectric device and phase change materials on the battery pack. The effect of arrangement and cooling / heating power for semiconductor thermoelectric devices on the thermal performance in different temperature ambient was investigated in this paper, as well as the time of heat preservation and the power consumption. The temperature range of the thermal management during the cooling and heating process was optimized. And the heat preservation effect of battery pack was studied when the pack was in the discharged and charged process in hot environment. At last the performance of pack after continuous cooling and heat preservation cycle was simulated to study the stability of this thermal management method. The main results are included:

(1) The combination of semiconductor thermoelectric device and phase change materials can keep the outdoor standby battery pack for base station at optimum temperature range for 4.4 days in the 323 K ambient after once cooling process and 3.52 days in the 263 K ambient after once heating process.

(2) When the semiconductor thermoelectric devices distributed at two flanks of minimum size direction, compared with other arrangement, the temperature uniformity and heat preservation time were improved. When the temperature difference between upper or lower

limit of thermal management temperature range and the T_{PCM} was no more than 5K, ΔT_{max} of battery module during the cooling or heating process was lower than 5K.

(3) As the cooling / heating power increased, the time of cooling / heating process and heat preservation process decreased. Considering the stability of semiconductor thermoelectric devices and the heat dissipation of hot end, the best choice of cooling power was 200W. In order to decrease the heating frequency and consumption, the battery pack heated with 200W was suitable. When the average ambient temperature was between 333K and 253K, the cooling / heating time decreased and the heat preservation time increased, as the ambient temperature got close to the phase change temperature of PCMs.

(4) After 1C discharging and 0.5C charging process, $T_{\max}$ of battery module was under the 312K, which did not exceed the optimal temperature range of lithium battery. During continuous cooling and heat preservation cycle, the time of battery module cooling process floated around 14 hours and the time of heat preservation process floated around 4.15 days when the average ambient temperature was 323K. The heat preservation effect of this thermal management method for outdoor standby battery pack was stable.

Acknowledge

The authors would like to thanks for supports by NSFC-RS (UK) [grant number 51611130199]; National Natural Science Foundation of China: No.51607176.

References

[1] C. Restrepo, A.Salazar, H. Schweizer, A. Ginart. Residential Battery Storage: Is the Timing Right, Electrification Magazine. 3(2015) 14-21

[2] F. Bai, M. Chen, W. Song, Z. Feng, Y. Li, Y. Ding. Thermal management performances of PCM/water cooling-plate using for lithium-ion battery module based on non-uniform internal heat source, Appl. Therm. Eng. 126 (2017) 17–27

[3] Yan Ji, Chao Yang Wang. Heating strategies for Li-ion battery module operated from subzero temperatures, Electrochim. Acta. 107 (2013) 664–674

[4] F. Bahiraei, A. Fartaj, G. Nazri. Electrochemical-thermal Modeling to Evaluate Active Thermal Management of a Lithium-ion Battery Module, Electrochim. Acta. 254 (2017) 59–71.

[5] Z. An, L. Jia, Y. Ding, C. Dang, X. Li. A Review on Lithium-ion Power Battery Thermal Management Technologies and Thermal Safety, J. Therm. Sci. 26 (2017) 391-412.

[6] G. Xia, L. Cao, G. Bi. A review on battery thermal management in electric vehicle application, J. Power Sources, 367 (2017) 90-105.

[7] Z. Rao, Z. Qian, Y. Kuang, Y. Li. Thermal performance of liquid cooling based thermal management system for cylindrical lithium-ion battery module with variable contact surface, Appl. Therm. Eng. 123 (2017) 1514–1522.

[8] M. Chen, F. Bai, W. Song, J. Lv, S. Lin, Z. Feng, Y. Li, Y. Ding, A multilayer electrothermal model of pouch battery during normal discharge and internal short circuit process, Appl. Therm. Eng. 120 (2017) 506–516.

[9] W. Song, M. Chen, F. Bai, S Lin, Y. Chen, Z. Feng, Non-uniform effect on the thermal/aging performance of Lithium-ion pouch battery, Appl. Therm. Eng. 128 (2018) 1165–1174.

[10] X. Zhang, X. Kong, G. Li, J. Li. Thermodynamic assessment of active cooling/heating

methods for lithium-ion batteries of electric vehicles in extreme conditions, Sol. Energy. 64 (2014) 1092-1101.

[11] X. Meng, Z. Lu, L. Jin, L. Zhang, W. Hu, L. Wei, J. Chai. Experimental and numerical investigation on thermal management of an outdoor battery cabinet, Appl. Therm. Eng. 91 (2015) 210-224.

[12] C. Cheng, S. Huang, T. Cheng. A three-dimensional theoretical model for predicting transient thermal behavior of thermoelectric coolers, Int. J. Heat. Mass. Tran, 53 (2010) 2001–2011.

[13] H.Y. Zhang, Y.C. Mui, M. Tarin. Analysis of thermoelectric cooler performance for high power electronic packages, Appl. Therm. Eng. 30 (2010) 561–568.

[14] Y. Liu, S. Yang, B. Guo, C. Deng. Numerical analysis and design of thermal management system for lithium ion battery pack using thermoelectric coolers, Adv. Mech. Eng. 2014 852712

[15] A. Ginart, A. Salazar, C. Restrepo, M. Geiger, H. Schweizer. Thermoelectrical Management System for Stationary Outdoor Lithium-ion Energy Storage, IEEE Green Technologies 2016.

[16] M. Malik, I. Dincer, M. Rosen. Review on use of phase change materials in battery thermal management for electric and hybrid electric vehicles, Int. J. Energ. Res. 40(2016) 1011–1031.

[17] Q. Wang, B. Jiang, B. Li, Y. Yan. A critical review of thermal management models and solutions of lithium-ion batteries for the development of pure electric vehicles, Renew. Sustain. Energy Rev. 64 (2016) 106–128.

[18] J Yan, K Li, H Chen, Q Wang, J Sun, Experimental study on the application of phase change material in the dynamic cycling of battery pack system, Energ. Conver. Manage. 128(2016) 12–19

[19] M. Malik, I. Dincer, M. Rosen, M. Fowler. Experimental Investigation of a New Passive Thermal Management System for a Li-Ion Battery Pack Using Phase Change Composite Material, Electrochim. Acta. 257 (2017) 345-355.

[20] S. Al-Hallaj, J. Selman, Thermal modeling of secondary lithium batteries for electric vehicle/hybrid electric vehicle applications, J. Power Sources 110 (2002) 341–349.

[21] N. Javani, I. Dincer, G.F. Naterer, G.L. Rohrauer, Modeling of passive thermal management for electric vehicle battery packs with PCM between cells, Appl.Therm. Eng. 73 (2014) 307–316.

[22] Z. Wang, H. Zhang, X. Xia. Experimental investigation on the thermal behavior of cylindrical battery with composite paraffin and fin structure. Int. J. Heat Mass Tran. 109 (2017) 958–970.

[23] J Yan, Q Wang, K Li, J Sun, Numerical study on the thermal performance of a composite board in battery thermal management system, Appl. Therm. Eng. 106 (2016) 131-140

[24] A. Cosentino. Thermal management of telecommunications battery module using phase change materials (PCM) Jacket, IEEE. 2000

[25] W. Wu, X. Yang, G, Zhang, K. Chen, S.Wang, Experimental investigation on the thermal performance of heat pipe-assisted phase change material based battery thermal management system, Energ. Conver. Manage. 138 (2017) 486-492

[26]Z. Rao, Q. Wang, C. Huang, Investigation of the thermal performance of phase change material/mini-channel coupled battery thermal management system, Appl Energ. 164 (2016) 659-669

[27] B. P. Jelle, Traditional, state-of-the-art and future thermal building insulation materials and

solutions – Properties, requirements and possibilities, Energ Buildings. 43 (2011) 2549–2563

[28] K. Onda, T. Ohshima, M. Nakayama, K. Fukuda, T. Araki, Thermal behavior of small lithium-ion battery during rapid charge and discharge cycles, J Power Sources. 158 (2006) 535–542.

[29] T. Hatchard, D. MacNeil, D. Stevens, L. Christensen, J. Dahnd, Importance of heat transfer by radiation in Li-ion batteries during thermal abuse, Electrochem Solid St, 3 (7) 305-308 (2000)

[30] D Jeon, S. Baek. Thermal modeling of cylindrical lithium ion battery during discharge cycle, Energ Conver Manage 52 (2011) 2973–2981.

[31] K. Smith, C. Wang, Power and thermal characterization of a lithium-ion battery pack for hybrid-electric vehicles, J Power Sources. 160 (2006) 662–673.

[32] L. Saw, Y. Ye, A. Tay, Electrochemical–thermal analysis of 18650 lithium iron phosphate cell, Energ Conver Manage. 75 (2013) 162–174.

[33] Y. Inui, Y. Kobayashi, Y.Watanabe, Y.Watase, Y. Kitamura. Simulation of temperature distribution in cylindrical and prismatic lithium ion secondary batteries, Energ. Conver. Manage. 48(2007) 2103–2109.

[34]Y. Cengel, A. Ghajar, Heat and Mass Transfer: Fundamentals & Applications, McGraw-Hill, NewYork, NY,USA, 4th edition, 2011.

Table captions

Table 1 Physical sizes and parameters used in simulation

Table 2 Volume fraction of solid state PCMs after cooling process

Table 3 Volume fraction of liquid state PCMs after heating process

Figure captions

Fig. 1 Schematic of the battery pack with semiconductor thermoelectric devices and PCMs

Fig. 2 Independent test of grid number (a), time step for cooling/heating process (b) and time step for heat preservation process (c)

Fig.3. Temperature of battery module with passive cooling versus time with different environment temperature, (a) average ambient temperature was 323K, (b) average ambient temperature was 263K

Fig.4 Arrangement of the semiconductor thermoelectric devices

Fig.5 (a)Temperature of monitoring point, (b) ΔT_{max} of the battery versus time in cooling process, (c) temperature of monitoring point, (d) ΔT_{max} of the battery versus time in heat preservation process in high temperature ambient

Fig.6 (a)Temperature of monitoring point, (b) ΔT_{max} of the battery versus time in heating process, (c) temperature of monitoring point, (d) ΔT_{max} of the battery versus time in heat preservation process in high temperature ambient

Fig.7 Temperature variation of battery module of case 3 in (a) cooling process, (b) heat preservation process in high temperature ambient, (c) heating process, (d) heat preservation process in low temperature ambient with the temperature range of thermal management between 296K and 306K, (e) ΔT_{max} of battery module in cooling/heating process, (f) ΔT_{max} of battery module in heat preservation process

Fig.8 (a) Time of cooling process and heat preservation process, (b) Power consumption, (c) Temperature difference in cooling process, (d) Temperature difference of the battery in high

temperature ambient versus different cooling power

Fig.9 (a) Time of heating process and heat preservation process, (b) Power consumption, (c) Temperature difference in heating process, (d) Temperature difference of the battery in high temperature ambient versus different heating power

Fig.10 Time of heating process and heat preservation process versus temperature; (a) in high temperature ambient, (b) in low temperature ambient

Fig.11 Temperature variation of battery module in discharge-charge process versus time; (a) discharged at the beginning of heat preservation process, (b) discharged at the beginning of cooling process

Fig.12 (a) $T_{\max}$ and ΔT_{max} of battery module, (b) time of cooling process and heat preservation process during continuous cooling and heat preservation cycle